Supplemental information for "Horizontal and vertical structure of reactive bromine events probed by bromine monoxide MAX-DOAS spectroscopy"

William R. Simpson*[1], Peter K. Peterson[2], Udo Frieß[3], Holger Sihler[4], Johannes Lampel[3,4], Ulrich Platt[3], Chris Moore[5], Kerri Pratt[2], Paul Shepson[6], John Halfacre[6, §], and Son V. Nghiem[7]

[1] Geophysical Institute and Department of Chemistry and Biochemistry, University of Alaska Fairbanks, Fairbanks, AK 99775, USA
[2] Department of Chemistry, University of Michigan, Ann Arbor, MI, USA
[3] Institute of Environmental Physics, University of Heidelberg, Heidelberg, Germany
[4] Max Planck Institute for Chemistry, Mainz, Germany
[5] Gas Technology Institute, Des Plaines, IL, USA
[6] Purdue University, West Lafayette, IN, USA
[7] Jet Propulsion Laboratory, California Institute of Technology, Pasadena, CA, USA
[§] Current address: Indiana University Southeast, New Albany, IN, USA

[*]*Correspondence to*: William R. Simpson (wrsimpson@alaska.edu)

17 February 2017

This analysis is based upon spectral fits using QDOAS software with the following settings. A common wavelength interval, from 337nm to 364nm, was used for both BrO and O_4 spectral fitting. Molecular absorbers were not allowed to shift with respect to the wavelength scale, and the rotational Raman scattering, aka "Ring" spectrum (Grainger and Ring, 1962) was constrained to be within 0.1nm of the reference spectrum, but was typically closer to zero shift. To account for the "tilt effect", the spectrum was allowed to shift with respect to the reference (Rozanov et al., 2011; Lampel et al., 2017b); these shifts were significantly smaller than one pixel. For the Avantes spectrometers (IL1 and IL2), no intensity offset was allowed, but for the Ocean Optics (model QE65000 in the BARC instrument), a constant offset was fitted to account for instrumental stray light, which was found to be significantly larger for the BARC instrument. The BrO absorption cross section was from Fleischmann and Burrows (2000) at 243K. The NO_2 cross section was from Voigt et al. (2002) at 260K. The O_4 absorption cross section was from Thalman and Volkamer (2013) at 273K. Additionally, the difference between the 253K and 293K O_4 cross sections was fitted to account for the temperature-dependent O_4 absorption shape. The ozone cross section was from Serdyuchenko et al. (2014) at 263K, and the temperature difference between ozone cross sections at 243K and 283K was used to account for temperature dependent absorption shape. The rotational Raman scattering (Ring) pseudo-absorber spectrum was calculated in DOASIS (Kraus, 2006) at 273K, and a Ring effect temperature dependence was calculated as the difference between 273K and 243K, as found in Lampel et al. (2017a). Table S1 shows fitting error statistics from the spectral retrievals. For use in the HeiPro optimal estimation fitting, the BrO fit error was multiplied by a factor of two following an estimate from Stutz and Platt (1996).

These figures show supplemental information discussed in the text. Figure S1 shows histograms of information content (DOFS) from BrO and O_4 OE fitting. Figure S2 shows wind direction statistics. Figure S3 shows correlation diagrams during the pre-lead opening period. Figure S4 shows histograms of the difference in BrO LT-VCD between sites. Figures

S5-S7 show aerosol extinction coefficient curtain plots for periods B1-B3, respectively. Figures S8-S10 show BrO curtain plots for periods B1-B3, respectively. Also provided is a supplemental animation that shows the measurement locations superimposed on sea ice images.

References:

Fleischmann, O. C. and Burrows, J. P.: BrO Spectra, [online] Available from: http://www.iup.uni-bremen.de/gruppen/molspec/databases/referencespectra/brospectra/index.html (Accessed 1 February 2017), 2000.

Grainger, J. F. and Ring, J.: Anomalous Fraunhofer Line Profiles, Nature, 193(4817), 762–762, doi:10.1038/193762a0, 1962.

Kraus, S.: DOASIS - A Framework Design for DOAS, University of Heidleberg., 2006.

Lampel, J., Pöhler, D., Polyansky, O. L., Kyuberis, A. A., Zobov, N. F., Tennyson, J., Lodi, L., Frieß, U., Wang, Y., Beirle, S., Platt, U. and Wagner, T.: Detection of water vapour absorption around 363 nm in measured atmospheric absorption spectra and its effect on DOAS evaluations, Atmos. Chem. Phys., 17(2), 1271–1295, doi:10.5194/acp-17-1271-2017, 2017a.

Lampel, J., Wang, Y., Hilboll, A., Beirle, S., Sihler, H., Pukite, J., Platt, U. and Wagner, T.: The tilt-effect in passive DOAS observations, Atmos. Meas. Tech., in preparation, 2017b.

Peterson, P. K., Simpson, W. R., Pratt, K. A., Shepson, P. B., Frieß, U., Zielcke, J., Platt, U., Walsh, S. J. and Nghiem, S. V: Dependence of the vertical distribution of bromine monoxide in the lower troposphere on meteorological factors such as wind speed and stability, Atmos. Chem. Phys., 15(4), 2119–2137, doi:10.5194/acp-15-2119-2015, 2015.

Rozanov, A., Kühl, S., Doicu, A., McLinden, C., Puķīte, J., Bovensmann, H., Burrows, J. P., Deutschmann, T., Dorf, M., Goutail, F., Grunow, K., Hendrick, F., von Hobe, M., Hrechanyy, S., Lichtenberg, G., Pfeilsticker, K., Pommereau, J. P., Van Roozendael, M., Stroh, F. and Wagner, T.: BrO vertical distributions from SCIAMACHY limb measurements: comparison of algorithms and retrieval results, Atmos. Meas. Tech., 4(7), 1319–1359, doi:10.5194/amt-4-1319-2011, 2011.

Serdyuchenko, A., Gorshelev, V., Weber, M., Chehade, W. and Burrows, J. P.: High spectral resolution ozone absorption cross-sections; Part 2: Temperature dependence, Atmos. Meas. Tech., 7(2), 625–636, doi:10.5194/amt-7-625-2014, 2014.

Stutz, J. and Platt, U.: Numerical analysis and estimation of the statistical error of differential optical absorption spectroscopy measurements with least-squares methods, Appl. Opt., 35(30), 6041, doi:10.1364/AO.35.006041, 1996.

Thalman, R. and Volkamer, R.: Temperature dependent absorption cross-sections of O2–O2 collision pairs between 340 and 630 nm and at atmospherically relevant pressure, Phys. Chem. Chem. Phys., 15(37), 15371, doi:10.1039/c3cp50968k, 2013.

Voigt, S., Orphal, J. and Burrows., J. P.: The temperature and pressure dependence of the absorption cross-sections of NO2 in the 250–800 nm region measured by Fourier-transform spectroscopy, J. Photochem. Photobiol. A Chem., 149, 1–7, 2002.

Tables:

Table S1: Fitting error statistics

Instrument	Fit RMS	Fit error (1σ) BrO / molecule cm^{-2}	Fit error (1σ) O_4 / $molecule^2$ cm^{-5}	Fit error (1σ) NO_2 / molecule cm^{-2}
IceLander1	3.7e-4	9.0e+12	4.2e+41	8.7e+14
BARC	3.6e-4	9.5e+12	4.1e+41	8.9e+14
IceLander2	2.7e-4	6.8e+12	3.0e+41	6.5e+14

Figures:

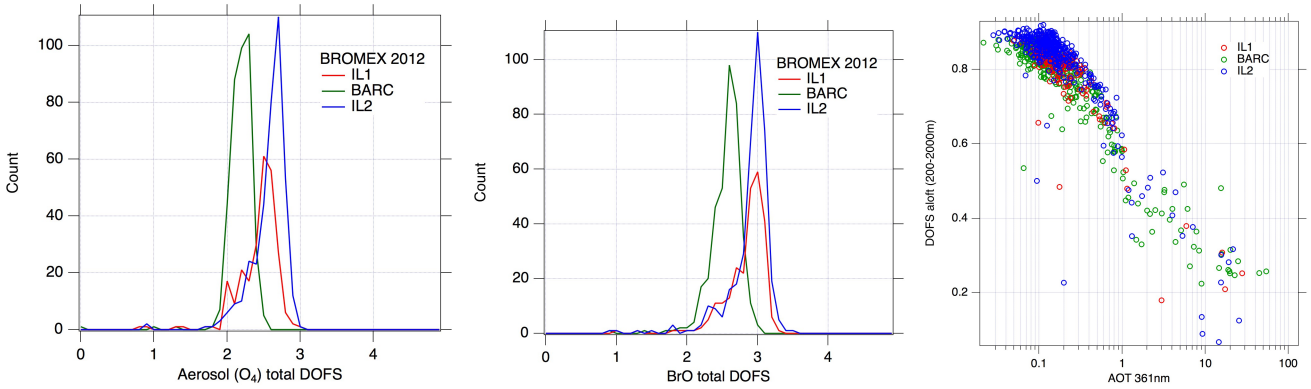

Figure S1: Histograms of degrees of freedom for signal (DOFS) for the "fine grid" at each site for aerosol extinction measurements (via O_4 absorption), left panel and BrO, middle panel. The right panel shows the relationship between the BrO DOFS aloft on the coarsened grid (200-2000m AGL) versus aerosol optical thickness (AOT) at 361nm. Points with BrO <0.5 DOFS aloft are considered too affected by light scattering and are cut from subsequent analysis, as described in the text and in Peterson et al. (2015).

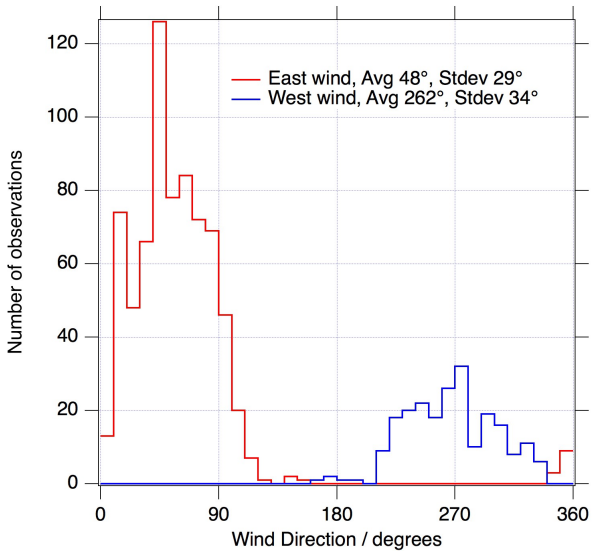

Figure S2: Histograms of wind direction at Barrow (Utqiaġvik), split into sectors as described in the text.

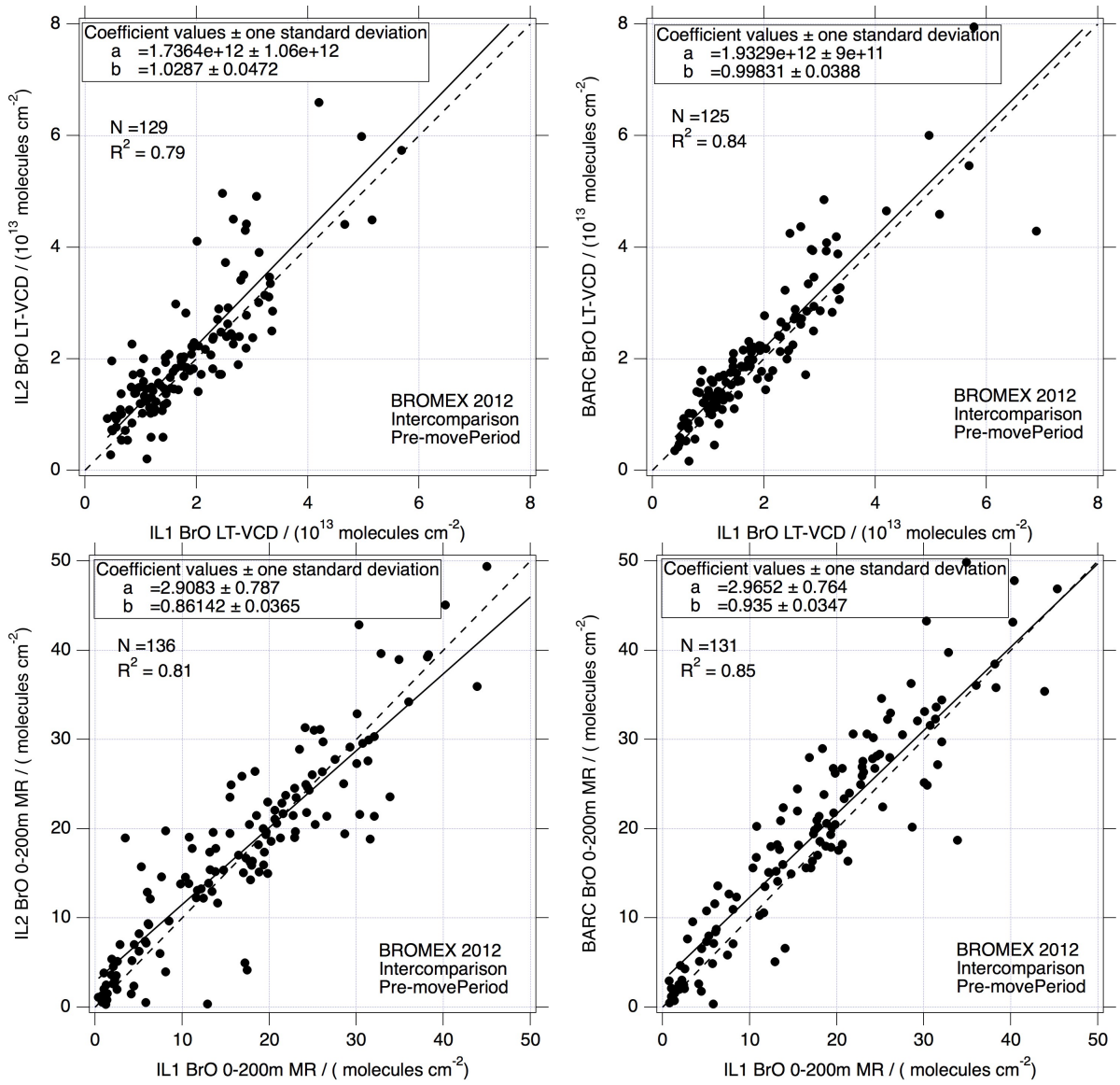

Figure S3: Correlation plots of BrO measurements (LT-VCD and 0-200m mixing ratio, MR) between sites during the period from March 9 to 23, after deployment of remote IL sites but before the sea ice lead breakage event when IL2 began moving downwind. For clarity, error bars are not shown, but are similar to those in Figure 3.

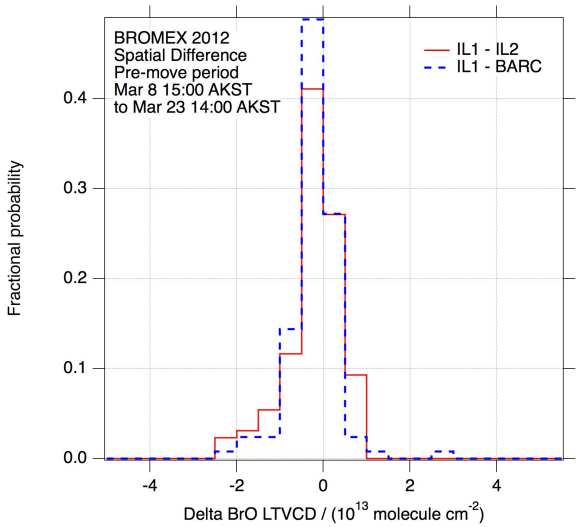

Figure S4: Histograms of the difference in BrO LT-VCD between sites. This difference is calculated from hourly data at each site in the period before the sea ice lead moved IL2, so there were no sea ice leads between sites. The probability of having a difference with absolute value less than 10^{13} molecule cm^{-2} is 89% for IL1-IL2, and 93% for IL1-BARC.

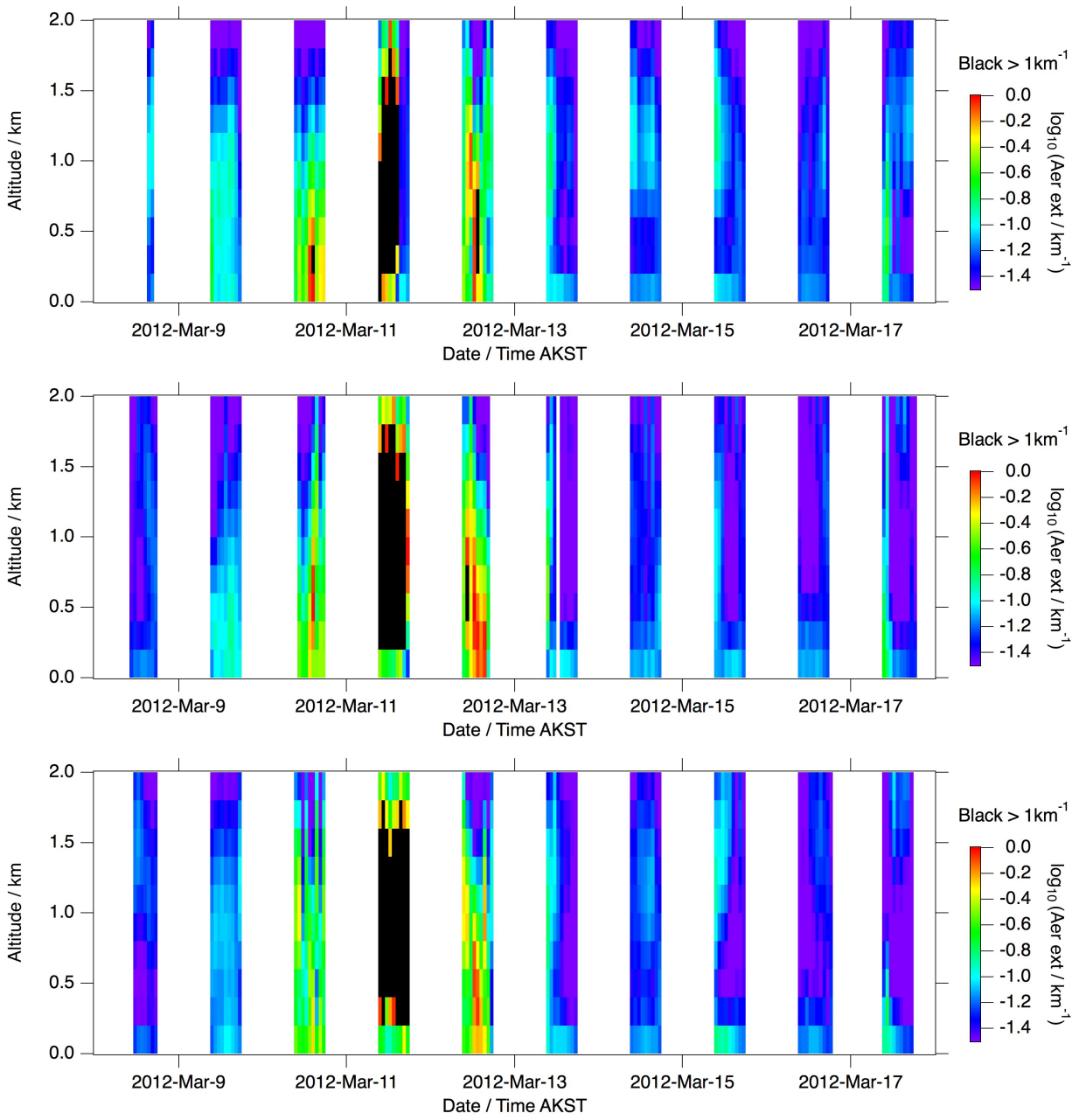

Figure S5: Aerosol extinction coefficient curtainplots for period B1. On all figures, the top panel is IL1, middle is BARC, and bottom is IL2. Values greater than 1 km^{-1} are represented as black, and features at higher altitude than these optically thick layers have little information content and should be ignored. White periods represent data gaps or nighttime, when measurements were not possible.

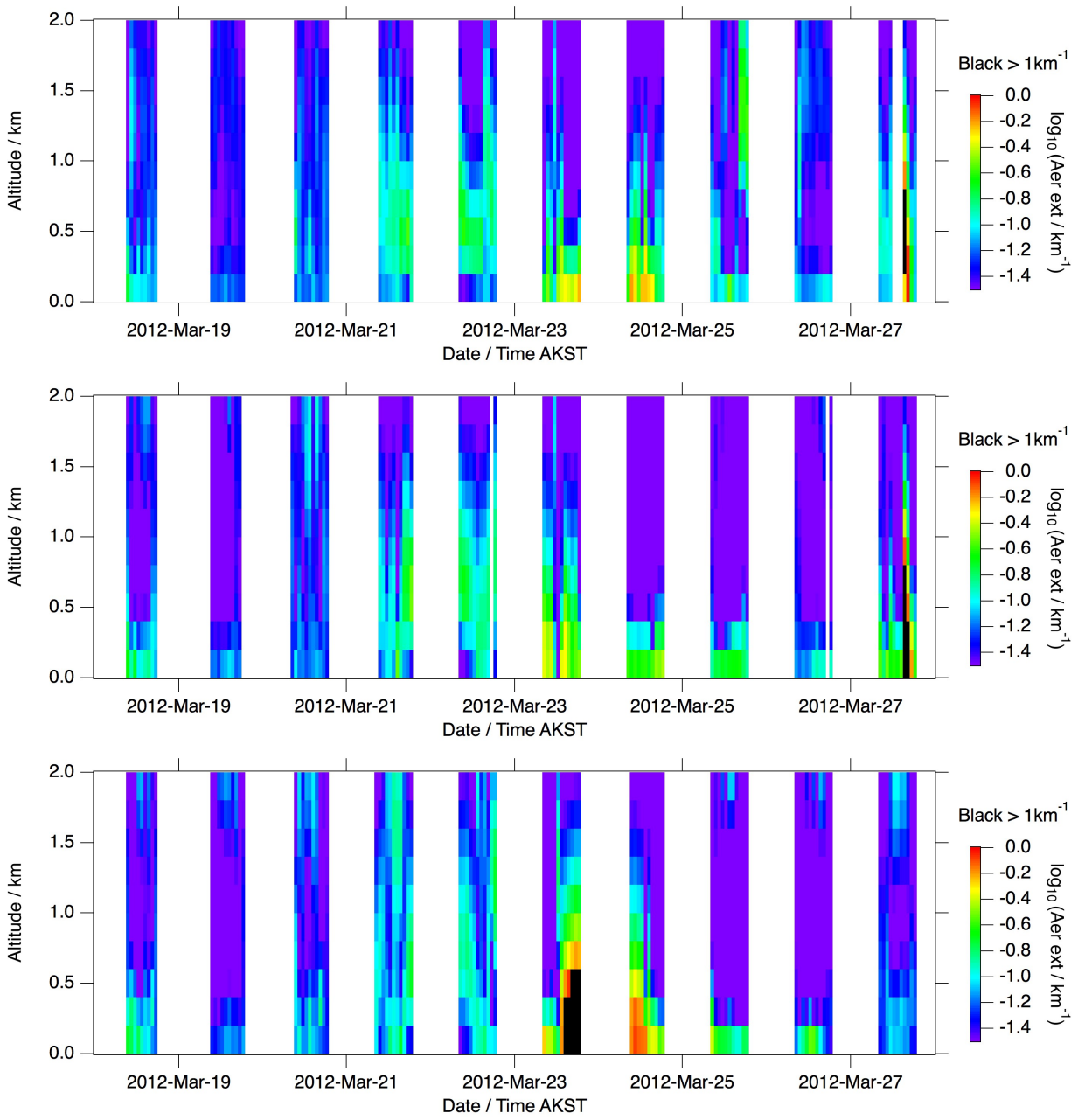

Figure S6: Aerosol extinction coefficient curtainplots for period B2.

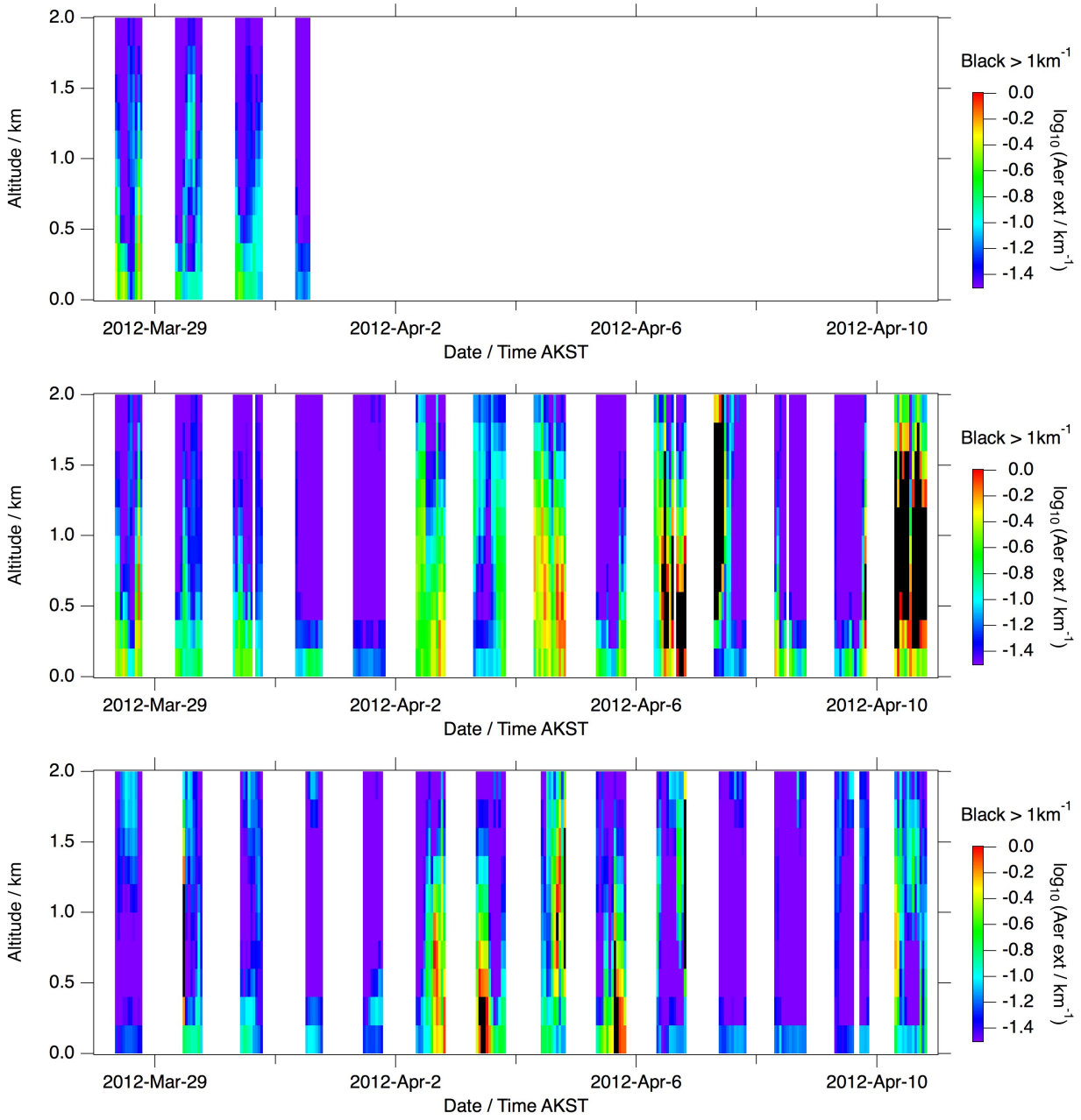

115

Figure S7: Aerosol extinction coefficient curtainplots for period B3.

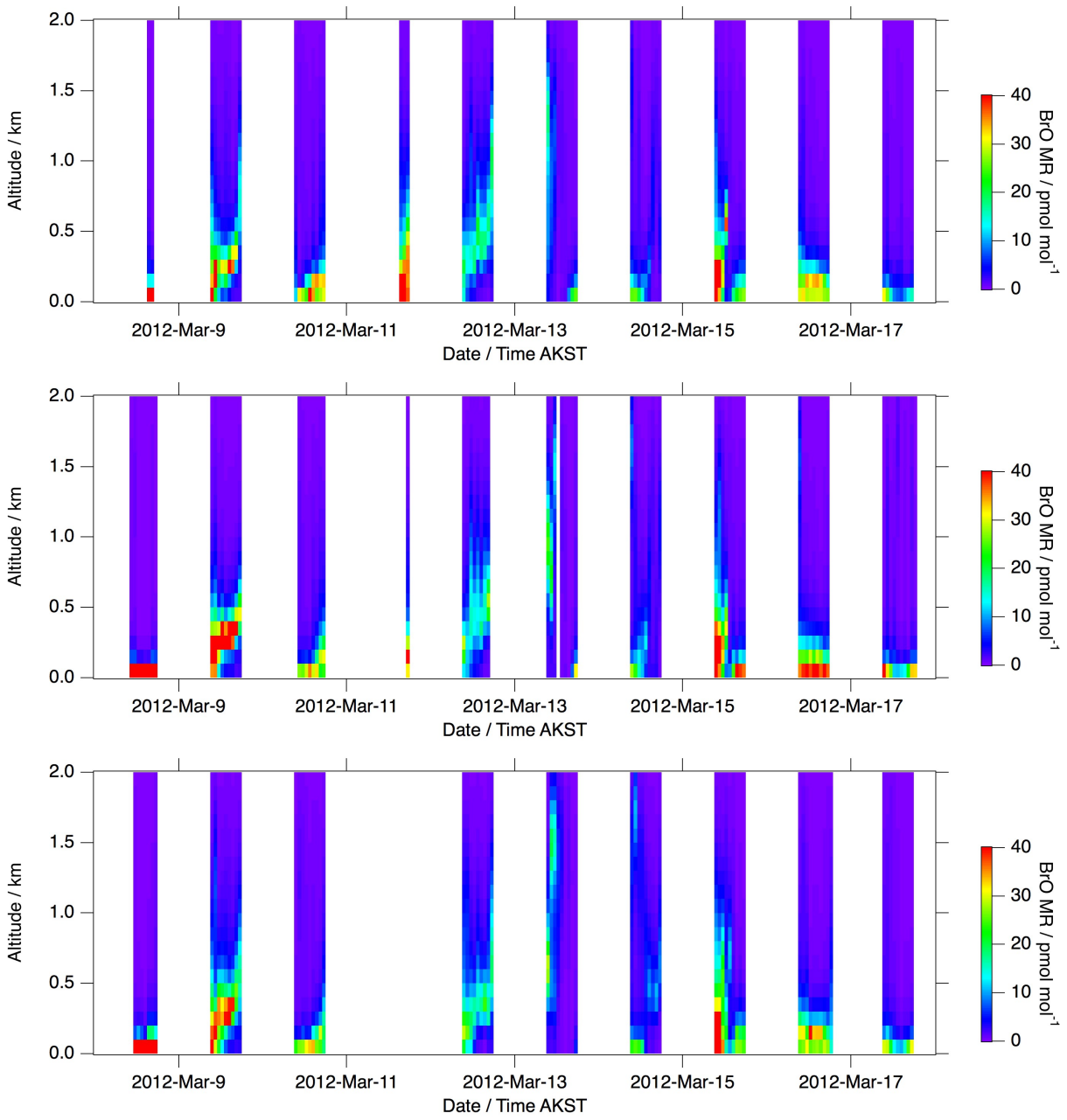

Figure S8: BrO mixing ratio (MR) curtainplots for period B1. On all figures, the top panel is IL1, middle is BARC, and bottom is IL2. Values greater than 40 pmol mol^{-1} in individual layers are probably caused by limited vertical resolution and are represented as the red color. White periods represent data gaps or nighttime, when measurements were not possible.

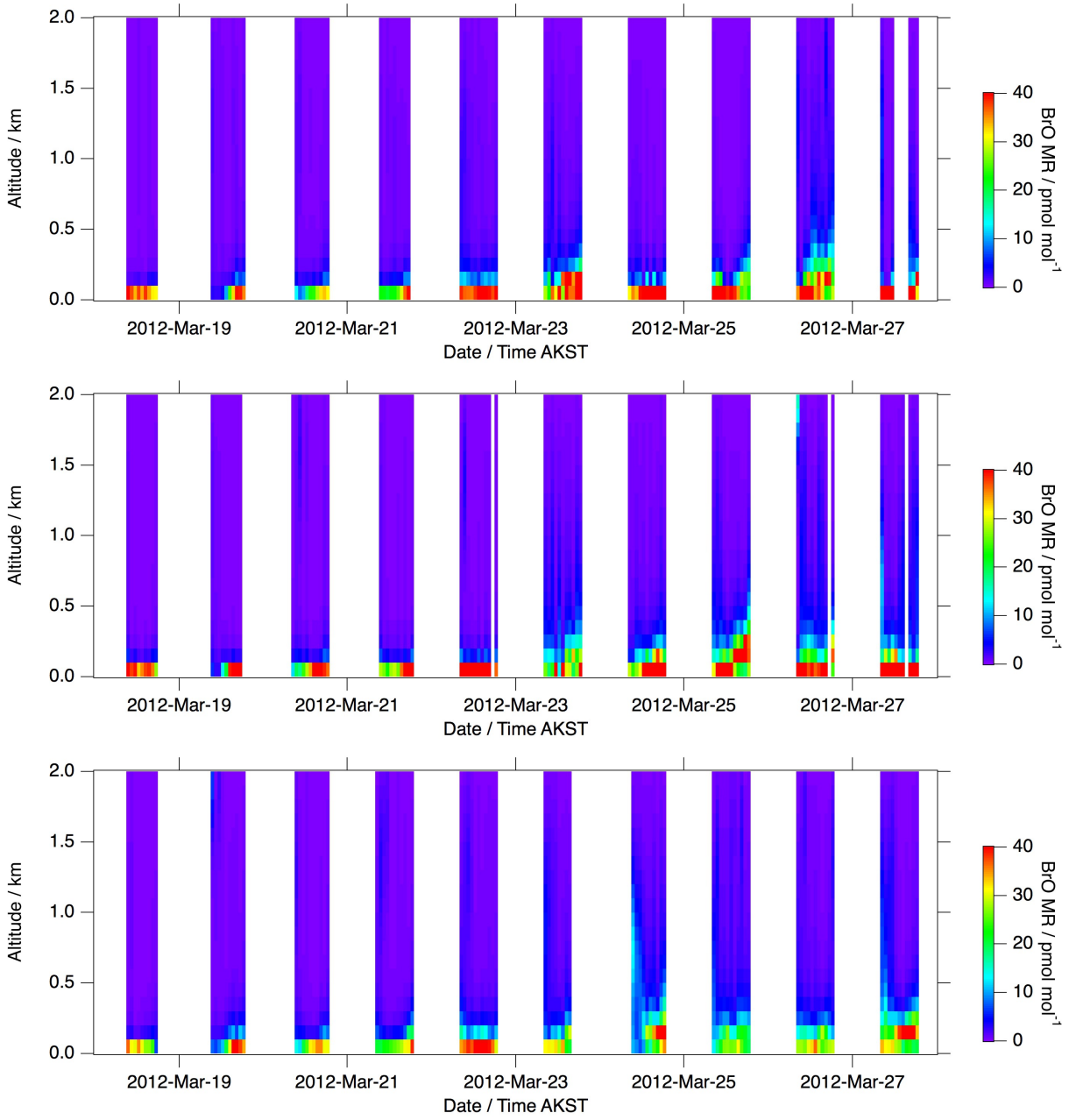

Figure S9: BrO mixing ratio (MR) curtainplots for period B2.

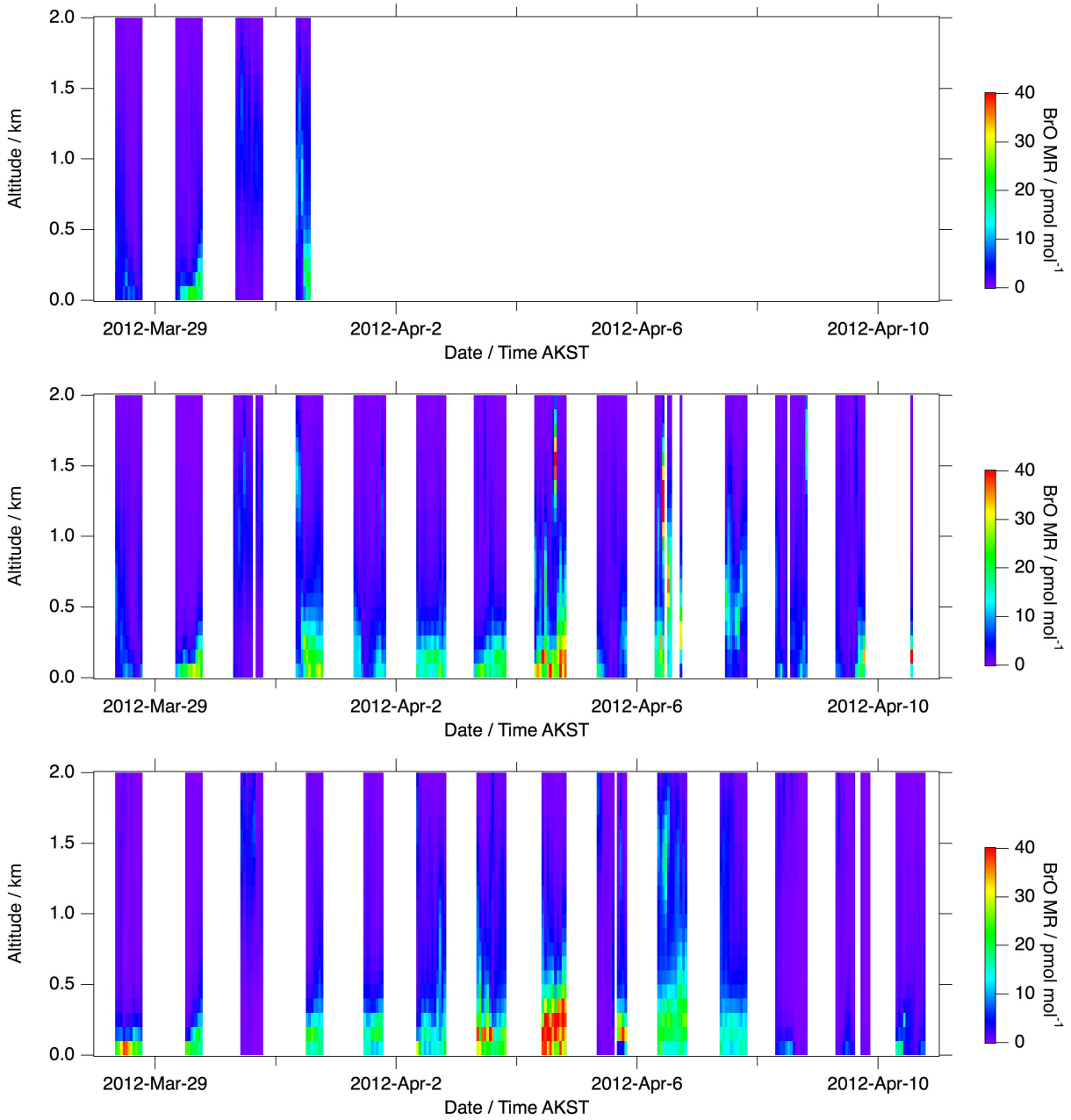

Figure S10: BrO mixing ratio (MR) curtainplots for period B3.